



Evaluation of effectiveness and resources consumption of water mist spray systems in Mediterranean areas by predictions based on LSTM Recurrent Neural Networks

Marco D'Orazio ^a, Costanzo Di Perna ^b, Elisa Di Giuseppe ^{a,*}, Gianluca Coccia ^b, Serena Summa ^c

^a Department of Construction, Civil Engineering and Architecture (DICEA), Università Politecnica delle Marche, via Brecce Bianche 12, Ancona 60100, Italy

^b Department of Industrial Engineering and Mathematical Sciences (DIISM), Università Politecnica delle Marche, via Brecce Bianche 12, Ancona 60100, Italy

^c Department of Science and Engineering of Materials, Environment and Urban Planning (SIMAU), Università Politecnica delle Marche, via Brecce Bianche 12, Ancona 60100, Italy

ARTICLE INFO

Keywords:

Evaporative cooling
Water mist spray
Neural Network
Outdoor thermal comfort
Urban heat mitigation
Resources consumption

ABSTRACT

To counter the increasing urban overheating, climate adaptation solutions are proposed. Among them, water mist spray recently acquired particular attention, due to its efficiency, cost-effectiveness, and versatility. However, spray devices require a large amount of water and energy to cool even limited areas, thus their environmental costs/benefits ratio should be carefully evaluated. This study analyses cooling benefits and resources consumption of mist devices in 11 cities within 3 climate contexts, through Recurrent Neural Networks (RNNs) trained with experimental data. RNNs predict the expected time series of thermal benefits and of energy and water consumptions, also considering different design solutions of devices. Results show that when sun/wind shielding is used in the sprayed area, or the height of nozzles is limited, higher cooling results are obtained. However, energy and water consumption are extremely high if misting systems are perennially active during the day. Considering all simulated conditions, the predicted average daily energy to obtain a unitary variation of the Mediterranean Outdoor Comfort Index is 4,17 Wh/m², while the corresponding average daily volume of water is 0,56 l*h/m². These results confirm the need for applications managed by control logics based on the acquisition of real-time climatic data to reduce the environmental loads.

1. Introduction

The year 2022 was one of hottest of the last century in Europe. Prolonged heat waves affected almost all countries, causing heat-related illness (Nishimura et al., 2021) and limiting the participation of the most vulnerable part of the population to the social life. In June, France activated red and orange alerts in 37 departments due to prolonged heat waves. Italy declared a state of emergency in five northern regions due to temperature increase and drought. In July, United Kingdom emanated an alert suggesting frailty people to reduce their external exposure during heat waves. Increase in air temperature and dryness also caused wildfires which affected large areas of Italy, Spain, France, Greece, and Portugal.

Considering that prolonged heat waves in such areas repeated almost every year for the last two decades, the development of overheating mitigation solutions became an important area of research interest

(Desert, Naboni, & Garcia, 2020), in order to allow outdoor access while reducing health risks for vulnerable population (Nishimura et al., 2021), especially elderlies. Among outdoor thermal mitigation methods, water mist spray recently acquired particular attention and is being more and more used in important architectural projects as well as in urban places, due to its ability to address both thermal and aesthetical issues (Farnham, Emura, & Mizuno, 2015; Li, Hong, Wang, Bai, & Chen, 2022; Meng, Meng, Gao, & Li, 2022; M Santamouris & Kolokotsa, 2016; M. Santamouris et al., 2017). The spray cooling process is based on evaporative cooling (Ulpiani, 2019) provided by water pulled into nozzles at high pressure (50–70 bar). The diameter and the cone of the nozzles vary depending on the type of application (Bao et al., 2019; H. Mao et al., 2021). Heat is removed by water mist systems mainly due to the phase change of the water and only additionally to the convective heat transfer of the fluid in motion. The heat and mass transfer mechanism has been analysed in detail by Kachhwaha, Dhar, and Kale (1998).

A literature review (Ulpiani, 2019) reported that several experiments

* Corresponding author.

E-mail address: e.digiuseppe@staff.univpm.it (E. Di Giuseppe).

Nomenclature			
C	State vector of the RNN	MOCI _{in}	MOCI value inside the misted area
F _t	Forget gate	MOCI _{out}	MOCI value outside the misted area
ICL	Thermal clothing insulation (clo)	RH	Relative humidity (%)
ID	Diffuse radiation (W/m ²)	RNN	Recurrent Neural Network
IS	Global solar radiation incident on the horizontal plane (W/m ²)	S _e	Amount of daily energy required to obtain a unitary variation of MOCI towards neutrality (Eq. (7))
I _{energy}	Total energy consumption during water mist use (Eq. (5))	S _w	Amount of daily water required to obtain a unitary variation of MOCI towards neutrality (Eq. (8))
I _{water}	Total water consumption during water mist use (Eq. (6))	T _A	Air Temperature (°C)
LCZ	Local Climate Zone	UC	“Undisturbed” conditions
LSTM	Long-Short-Term-Memory	UWG	Urban Weather Generator
MC	“Misted” conditions	VAR _{MOCI}	Water mist performance index (defined in Eq. (4))
MOCI	Mediterranean Outdoor Comfort Index	W _D	Wind Direction (°)
		W _S	Wind speed (m/s)

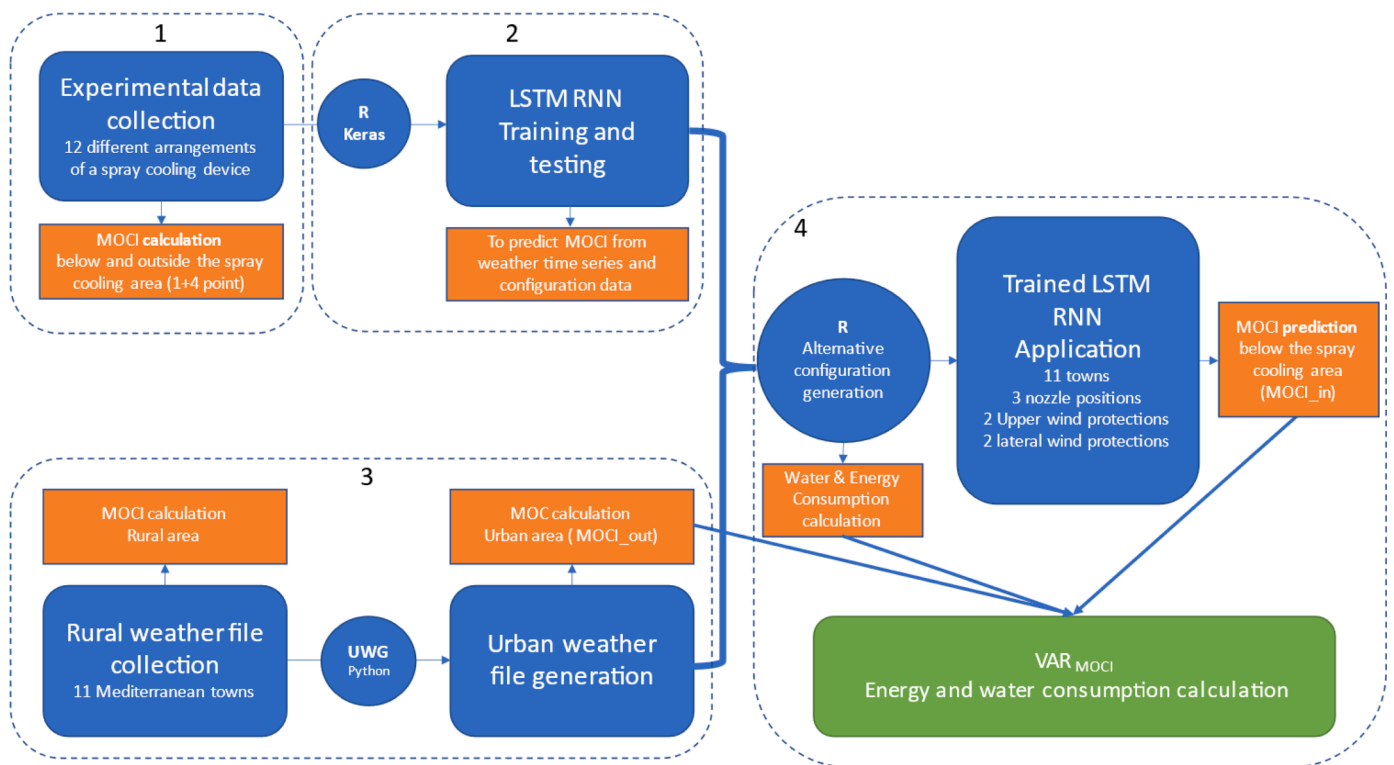


Fig. 1. Research framework.

have been performed to check the efficiency and efficacy of the water mist spray as a microclimate mitigator in specific contexts. Studies are mainly concentrated in temperate and humid climates (75% of the total), such as Csa (hot-summer Mediterranean) and Cfa (subtropical) climates, according to Koppen–Geiger classification. Research has been also performed in Cfb (temperate oceanic) climates, due to the increase of heat waves phenomena also in these areas, usually characterized by moderately warm summers. Only few studies were realised in semi-arid and tropical climates (Bwh, Af and Aw) (Zheng, Yuan, Wong, & Cen, 2019).

The ability of spray cooling devices to act as thermal stress mitigators mainly depends on two groups of interrelated factors: (1) technological features including (but not limited to) nozzle design and arrangement, water pressure, and type of control; (2) climatic context, including (but not limited to) local water vapour pressure, air temperature, wind speed and direction.

Concerning the technological factors, it has been reported that nozzle design, determining the average size of the droplets, strongly affects the performance of the technology. In particular, Ulpiani et al. analysed the influence of the average size of sprayed droplets, showing that an increase in droplets size affects the cooling potential and causes an unjustified increase in water and energy consumption (Ulpiani, Di Giuseppe, Di Perna, D’Orazio, & Zinzi, 2019b). Studies were also performed to check the influence of the systems activation controllers. Literature shows that a timed control allows to better handle the humidification gain and track specific comfort targets. Water temperature was also investigated, leading to the conclusion that its impact is very limited (Farnham, Nakao, Nishioka, Nabeshima, & Mizuno, 2015). Nozzle number and arrangement were also analysed, e.g. considering vertical and pointing downwards settings (Ulpiani, Di Giuseppe, Di Perna, D’Orazio, & Zinzi, 2019a). Among climatic factors, temperature, relative humidity and wind speed were especially addressed. It was

Table 1
Main configuration settings with design alternatives and recorded mean consumption values.

Technological variables and main configuration settings	Values
Nozzle height (from the ground)	2.2, 2.6, 2.9 m
Presence of vertical wind protection shielding	True, false
Presence of horizontal sun protection shielding	True, false
Functioning time	From 9.00 to 19.00 every day
Recorded mean water consumption	0.028 l/s when the device was on
Recorded energy consumption	740 Wh when the device was on



Fig. 2. Experimental test rig.

ascertained that the cooling effect is more relevant in still air, especially in case of micro-nebulization, due to the dilution caused by wind (Di Giuseppe et al., 2021; Ulpiani, 2019).

However, despite the amount of research in this field, there are still relatively unexplored issues. In particular, the environmental sustainability of the technology has been not widely investigated, despite the large amount of water and energy required to moist and cool the air in outdoor spaces. In order to find a proper balance between thermal benefits and environmental costs, spray cooling systems can be controlled and used only for limited periods and in limited outdoor area (Vanos et al., 2022). Optimisation solutions balancing mitigation needs and resources savings should be then further investigated.

This study provides a contribution in this direction. It presents optimisation rules based on the ratio between mitigation benefits and resources consumption, through the application of trained Long-Short-Term-Memory Recurrent Neural Networks (LSTM RNNs). LSTM RNNs have been trained with data coming from long experimental activities performed on a water mist spray system in different daily weather conditions and with different technological arrangements (concerning nozzle height and the presence of wind/sun protection devices). RNNs are able to predict the expected time series of the thermal benefits, expressed as MOCI (Mediterranean Outdoor Comfort Index) and the energy and water consumptions. They were then applied in 11 different urban contexts, covering Csa, Csb and Bsk Koppen-Geiger climates characterizing the Mediterranean areas, and with different technological and design arrangements (nozzle position, presence of sun/wind

shieldings, activation time). The variation of MOCI under the sprayed area compared to an undisturbed area has been taken as a benefit measure and compared to the energy and water needs.

2. Methodology

2.1. Research framework

The research activity entailed four main steps: (1) collection of experimental data on a spray cooling device considering different technological and design arrangements, and consequent MOCI calculation Section 2.2; (2) LSTM RNNs development, training and testing from experimental data Sections 2.3; (3) generation of “urban weather data” starting from “rural weather data” and calculation of MOCI values in “undisturbed” conditions (UC) Sections 2.4; (4) application of the trained RNNs to predict MOCI values in the “misted” conditions (MC), in both urban and rural areas, with alternative configurations of spray systems, and evaluation of the thermal benefits in respect to environmental costs (energy and water consumption) (Section 2.5). Fig. 1 schematically represents the research framework, described in detail in next sections.

2.2. Experimental data collection and MOCI calculation

Experimental data refers to a campaign performed during summer 2021 in Ancona, a middle town located in central Italy (Csa Koppen-Geiger climate), and extensively documented by the authors in Coccia et al. (2023). The following reports a summary of performed activities and obtained results.

A spray cooling device was tested for three months, from June to August, considering different technological alternatives (nozzle height, presence of wind/sun protection devices) to evaluate their impact on the system efficiency. Table 1 resumes the tested configurations.

A grid of 24 nozzles was installed on a metal frame structure to realize a 6×4 m sprayed area. The horizontal distance between the nozzles was set to 1 m (x and y-direction). The vertical distance of the nozzles from the ground was changed during the experimental activity. Three heights were considered (2.2, 2.6, and 2.9 m) to evaluate how the vertical distance of the nozzles from the human body can influence the perceived cooling effectiveness. Considering that wind and sun presence affects spray cooling performance (Ulpiani, 2019), two protection devices were tested. The first was a 4×2.9 m shielding vertically put on the most wind-exposed side. The second was a 6×4 m shielding horizontally located to protect the upper part from solar irradiation.

The water mist device is composed of 24 inox nozzles (0.2 mm diameter), with anti-drip systems, 1/4" tubes, and a pump characterized by a flow rate of 3 l/min and a working pressure of 70 bar. A melt-blown filtering unit ($5 \mu\text{m}$) was also installed. Electrical energy has been supplied by a PV grid (1.2 kWp), connected to an Edison 3024 inverter and 4 batteries (Prime AGM Deep Cycle 150 Ah 12 V). The activation cycle of the system was controlled by a relay connected to the pump and by a flow sensor (Kemor M152 Rain detector). The energy required by the pump and the water flow has been continuously measured. To evaluate the effectiveness of the spray cooling device, weather data were collected outside and inside the spray cooling area, i.e. in the UC and MC. A weather station (LASTEM-LSI) was installed far away from the spray cooling area to avoid any possible interaction. It collected the following parameters: Air Temperature (T_A), Relative Humidity (RH), Diffuse radiation (I_D), Wind Speed (WS) and Wind Direction (WD). Global solar radiation incident on the horizontal plane (IS) was recorded by means of a Hukseflux pyranometer. Under the nebulised area, 4 micro-climatic stations were installed. Each station included a T_A /RH sensor (PCMini52 – Mitchell: RH accuracy: $\pm 2\%$; T accuracy: $0.2 \text{ }^\circ\text{C}$) covered by a 13 mm HDPE protection head. Type T thermocouples were also installed at different heights to collect information about the vertical temperature profile. A globe-thermometer was installed in a corner

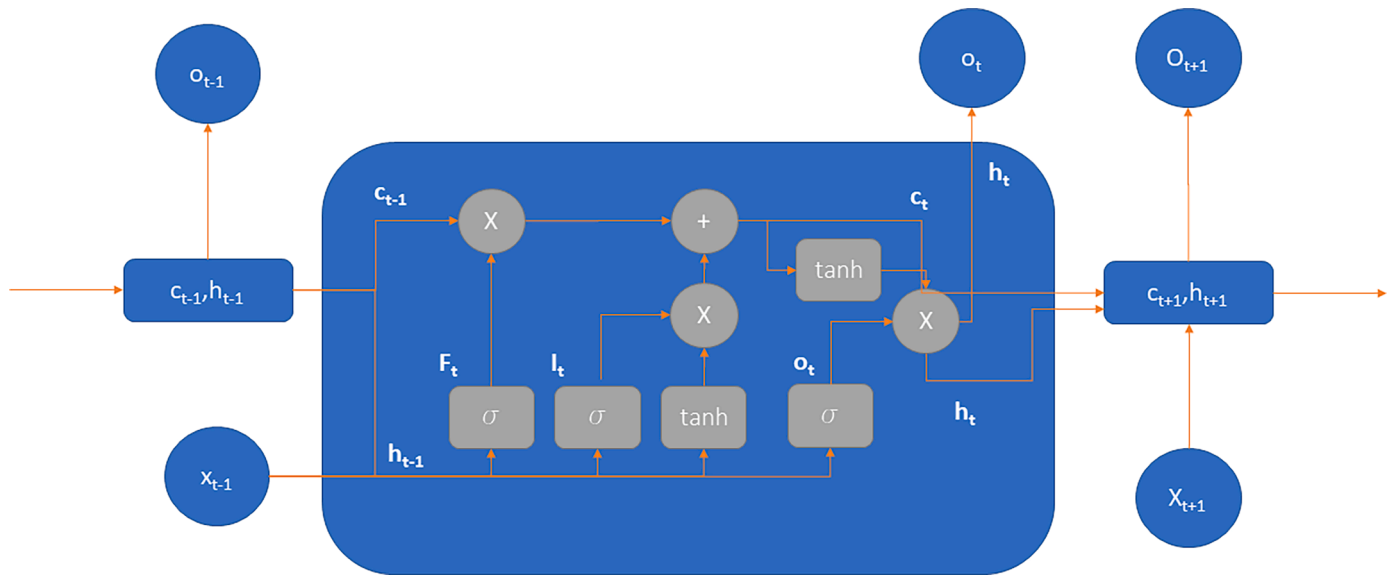


Fig. 3. Representation of the structure of a LSTM unit.

Table 2
Parameters characterising LCZ2 and assumed values according to Oke et al. (2017).

Parameter	Units	Range	Assumed value
Mean building height	m	10–25	10
Building density	–	0.4–0.7	0.5
Vertical to Horizontal (Canyon aspect ratio) ¹	–	0.75–2	0.8
Grass coverings	–	not available	0.1
Tree coverings	–	not available	0.1
Road albedo	–	not available	0.1
Vegetation albedo	–	not available	0.25
Sensible anthropogenic heat ²	W/m ²	< 75	20
Proportion of Mid-Rise apartments	%	not available	80
Proportion of Large offices	%	not available	20

¹ The canyon aspect ratio is the ratio of the mean height of buildings to the mean street width.

² Anthropogenic heat is the heat released per area as a result of human activities.

of the box. NI C-Series boards were used to continuously collect all data (12 s rate). Fig. 2 shows the installed spray cooling devices during a preliminary test and the installed weather station in the undisturbed area.

The results of the experimental campaign were discussed in the previous work of the authors (Coccia et al., 2023), then excluded from the present study.

Based on the collected experimental data, MOCI index has been calculated in 5 different positions (4 under the misted area and 1 in UC), to express the efficacy of the spray cooling system. MOCI is an outdoor comfort index developed for Mediterranean areas and also tested for spray cooling devices (Falasca, Curci, & Salata, 2021; Salata, Golasi, de Lieto Vollaro, & de Lieto Vollaro, 2016). It is based on the ASHRAE 7-points scale (+3= “hot”; +2= “warm”; +1= “slightly warm”; 0= “neutral”; -1= “slightly cool”; -2= “cool”; -3 = “cold”) and predicts the mean value of the votes that Mediterranean people might give

to judge the thermal qualities of an outdoor environment. MOCI was calculated based on the formulation proposed by Falasca et al. (2021):

$$MOCI = -4.257 + 0.325 \cdot I_{CL} + 0.146 \cdot T_A + 0.005 \cdot RH + 0.001 \cdot I_S - 0.235 \cdot WS \quad (1)$$

where T_A is the outdoor air temperature (°C), RH is the relative humidity of air (%), I_S is the global solar irradiation incident on the horizontal plane (W/m²) and WS is the wind speed (m/s). I_{CL} is the thermal clothing insulation (clo), which can be expressed as a function of the outdoor temperature T_A (Falasca et al., 2021):

$$I_{CL} = 1.608 - 0.038 \cdot T_A \quad (2)$$

The MOCI index can then be rewritten as function of the only outdoor temperature T_A , relative humidity RH, total incident radiation I_S and wind speed WS:

$$MOCI = -3.734 + 0.133 \cdot T_A + 0.005 \cdot RH + 0.001 \cdot I_S - 0.235 \cdot WS \quad (3)$$

The MOCI value outside the misted area ($MOCI_{out}$), i.e. in UC, was directly calculated from data collected by the weather station. The MOCI value inside the misted area ($MOCI_{in, mean}$), i.e. in MC, was calculated as the average value of 4 MOCI indices calculated in correspondence to the 4 micro-climatic stations inside the sprayed area ($MOCI_{in,1}$, $MOCI_{in,2}$, $MOCI_{in,3}$, $MOCI_{in,4}$).

2.3. Neural Network testing and training

In order to generalize the experimental data, which referred to a specific location, LSTM RNNs have been trained based on the collected data concerning weather conditions inside and outside the misted areas, as well as the configuration parameters of Table 1, and the installed mist performance results.

A LSTM RNN is a particular type of Neural Network, a well-known Machine Learning method which works to minimize the mean square error between the predicted output and the expected value (Singh, Singh, & Kumar, 2014). A NN comprises several layers and each layer is composed of one or more nodes, receiving inputs and sending outputs based on the weight assigned to each node. During the training process, the weight of each node is changed to minimize the prediction error. Then, the NN is directly trained from the data, based on the prediction errors.

RNN have been introduced because in some cases it is necessary to

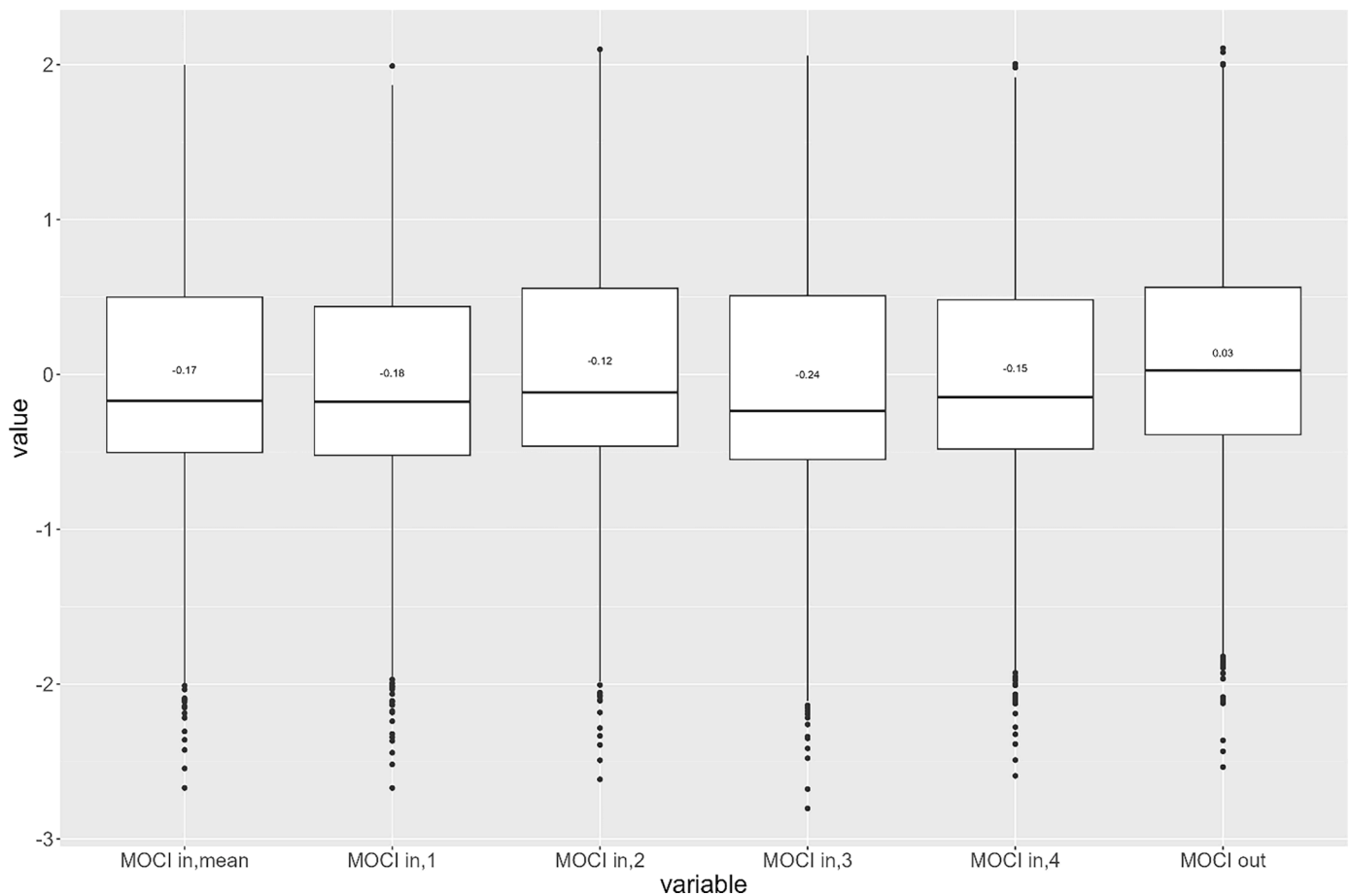


Fig. 4. Boxplot of MOCI values calculated in UC (MOCI_{out}) and in MC in different points and their average value (MOCI_{in,mean}).

understand how the prediction is influenced by the sequence of data and not only by the data themselves (Cohen et al., 2021). LSTM are RNNs that can learn long-term dependencies between time steps of sequence data with loops, allowing information to persist. LSTM has been frequently used for the recognition of speech and natural writing (Burak Gunay, Shen, & Newsham, 2019). LSTM are arranged in cell units, producing new outputs based on the current inputs and outputs and on the memory of the previous steps. At each output generated, each unit can modify the state vector «C» by adding or subtracting information through gates. The first gate is the «forget gate» (F_t) and is used to define the amount of information coming from the previous state to include in the process. The second gate is the «input gate» (I_t) and is used to define the «C» values to modify. After this process, predictions are generated. Fig. 3 shows the structure of the LSTM unit.

To train the LSTM RNN, time series of the weather data recorded in the UC (T_A , RH, I_S , WS) and necessary for MOCI calculation, as well as numerical and Boolean variables expressing the apparatus configurations (on/off, upper protection on/off, lateral protection on/off, height of the nozzles) were used as predictors, for a total of 8 parameters. The time series of the calculated MOCI values in the MC for the different configurations were used as variables to predict. To perform the training process, the dataset has been divided into two parts: «training» (50% of the values) and «testing» (50% of the values). Considering the number of predictors, the input shape was put to 8, the input layer was put to 64 nodes, the output layer to 1 node, corresponding to the number of predicted parameters and the hidden layer to 32 nodes, for a total of 2305 parameters. The number of epochs was put to 300. Each «epoch» measures the number of times that the learning algorithm works through the entire training dataset. Results were analysed through the following indicators: «loss», and «mean absolute error» (Gonçalves, Araújo,

Benevenuto, & Cha, 2013; Ribeiro, Araújo, Gonçalves, André Gonçalves, & Benevenuto, 2016). The LSTM Neural Network training and testing process has been performed through *R statistics rel.4.3*, writing a specific script based on the «Keras» python library and «reticulate» R package to access python packages. At the end of the process, a Neural Network able to predict the expected hourly time series of MOCI_{IN} has been derived based on the predictors (T_A , RH, I_S , WS, on/off, upper protection, lateral protection, height of the nozzles from the ground).

2.4. Urban weather data creation

To apply the trained LSTM RNN to different climatic conditions and locations, a set of 11 «urban hourly weather data» corresponding to Csa, Csb and Bsk climatic zones (according to Köppen–Geiger classification) has been generated. These three climatic zones were chosen as the most representative of the Mediterranean context in terms of dimension. Three towns are in Italy (Csa: Palermo, Rome; Csb: Bologna), four towns are in Spain (Bsk: Madrid, Zaragoza, Valencia; Csa: Granada) and one town is respectively in Greece (Csa: Athens), France (Csb: Nice) and Serbia (Csb: Belgrade). Towns have been selected to ensure representativity for latitude and longitude. To create the «urban hourly weather data», UWG (Urban Weather Generator) software has been used (Bueno, Nakano, & Norford, 2015). UWG is an open source validated tool (Boccalatte, Fossa, Gaillard, & Menezzo, 2020; Bueno et al., 2015; Litardo et al., 2020; J. Mao, Fu, Afshari, Armstrong, & Norford, 2018; Nakano, Bueno, Norford, & Reinhart, 2015), able to generate «urban weather» files, considering the main parameters affecting the urban micro-climate (building density, building height, anthropogenic heat, surface albedo, etc.), starting from «rural weather» data. The urban model entailed morphological and physical parameters corresponding

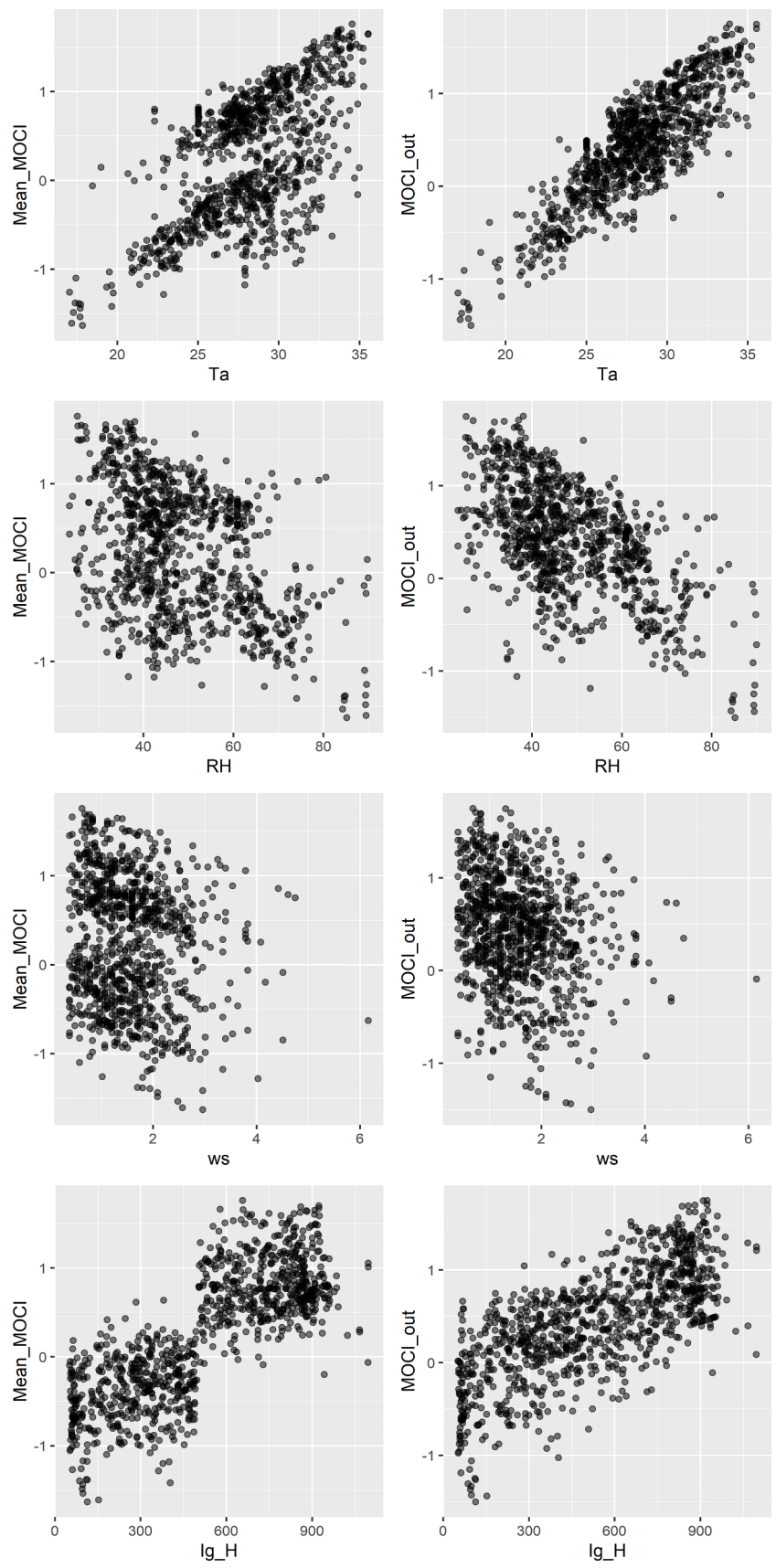


Fig. 5. Scatterplots of $MOCl_{in}$ and $MOCl_{out}$ vs T_a , RH, I_s , WS.

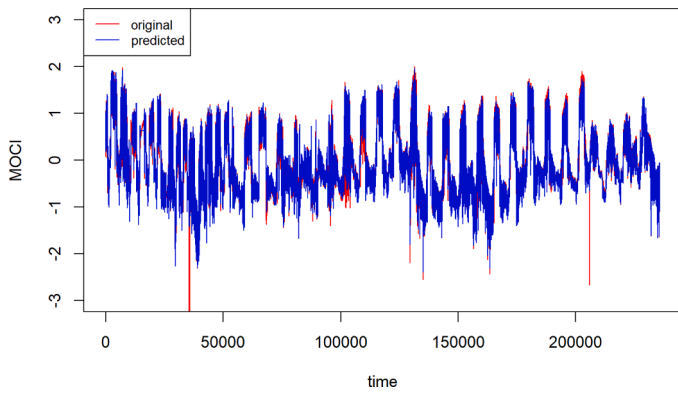


Fig. 6. Original and predicted MOCI values. Predictions were obtained through the trained LSTM RNN.

to the Local Climate Zone (LCZ) 2 (Maracchini, Bavarsad, Di Giuseppe, & D'Orazio, 2023; Oke, Mills, Christen, & Voogt, 2017), widely present in Mediterranean towns, characterized by high building densities. Indeed, LCZ 2 (compact midrise) is characterized by high canyon aspect ratios. Table 2 resumes the LCZ 2 parameters ranges and the related values assumed in the model.

Considering the input values reported in Table 2, and assuming a portion of the town characterized by residential buildings (80%) and offices (20%), a set of 11 hourly urban weather files in June-September period of each location has been generated in EPW format, starting from the corresponding rural weather files (data coming from weather stations near the town). Each EPW file includes 36 parameters. Among them, hourly data referring to the parameters measured during the experimental activity, and chosen as NN predictors, were extracted (T_A , RH, I_s , WS). Hourly weather data were combined with those describing the 12 alternative configurations of the spray cooling device (3 nozzle heights \times 2 upper shielding conditions \times 2 side shielding conditions, see Table 1). Then, the 12 configurations were tested in each of the 11 chosen cities, in both rural and urban areas. A total number of 264 alternative datasets was then obtained.

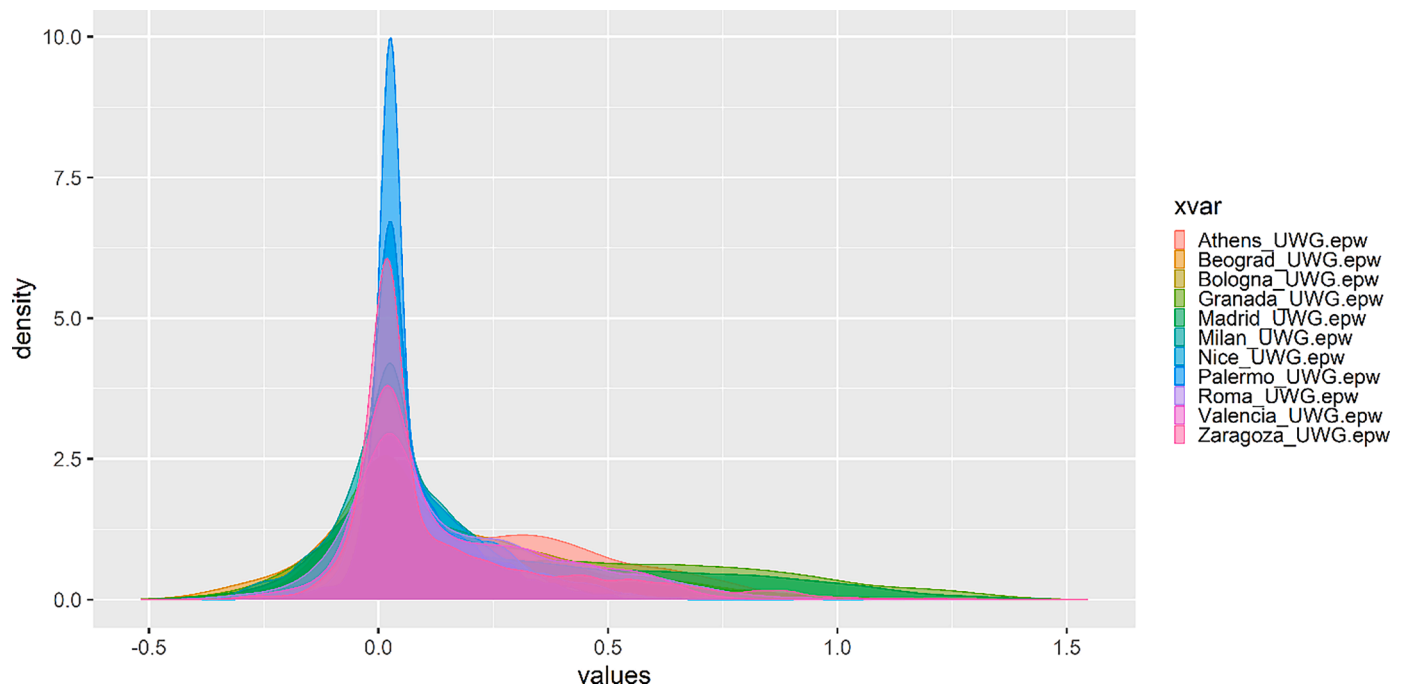


Fig. 7. Distributions of calculated differences in MOCI value of urban and rural areas for the 11 considered towns.

2.5. Application of the trained Neural Network and analysis of the results

The trained LSTM RNN was then used to predict the $MOCI_{in}$ time series in the period June-September (120 days) based on the data corresponding to each dataset. The water mist system was considered continuously active for 9 h/day. However, considering that the mist cooling device is useful with harsh external conditions due to overheating, only the periods with $MOCI_{out} > 1$ (Warm and Hot) were considered to calculate the effectiveness of the system and related energy and water consumption.

Then, for each location, a system effectiveness index, defined VAR_{MOCI} , has been then calculated as the sum of the hourly differences between the MOCI values calculated in the undisturbed and in the sprayed area when the cooling system is active (and $MOCI_{out} > 1$):

$$VAR_{MOCI} = \sum_{hours = 1}^n (MOCI_{in} - MOCI_{out}) \quad (4)$$

where n is the number of hours when $MOCI_{out}$ is > 1 .

Then, VAR_{MOCI} expresses the obtained cumulative benefits. The VAR_{MOCI} sign expresses the direction of the benefits: “-” from hot to cold; “+” from cold to hot.

The total resources consumptions of the spray cooling device (I_{energy} , I_{water}) during the operative phase were calculated for each configuration by multiplying “ m ” (hours of spray activity) by the hourly energy and water consumption per square meter, as follows.

$$I_{energy} = m \cdot (Hourly \ energy \ consumption) \ [kWh / m^2] \quad (5)$$

$$I_{water} = m \cdot (Hourly \ water \ consumption) \ [liters / m^2] \quad (6)$$

Hourly energy and water consumption values corresponding to the experimental setting were used to calculate I_{energy} and I_{water} , and they correspond to 0.031 kWh/m^2 and $4.75 \text{ l}^*/\text{h/m}^2$. A continuous use of the spray cooling system during each hour was assumed, considering limited differences of consumption results obtained during the experimental activity with continuous and intermittent activation (20 s on, 20 s off) without shieldings. Indeed, compared with the continuous activation, the relevant reduction of the cooling effect (-60%) obtained with the

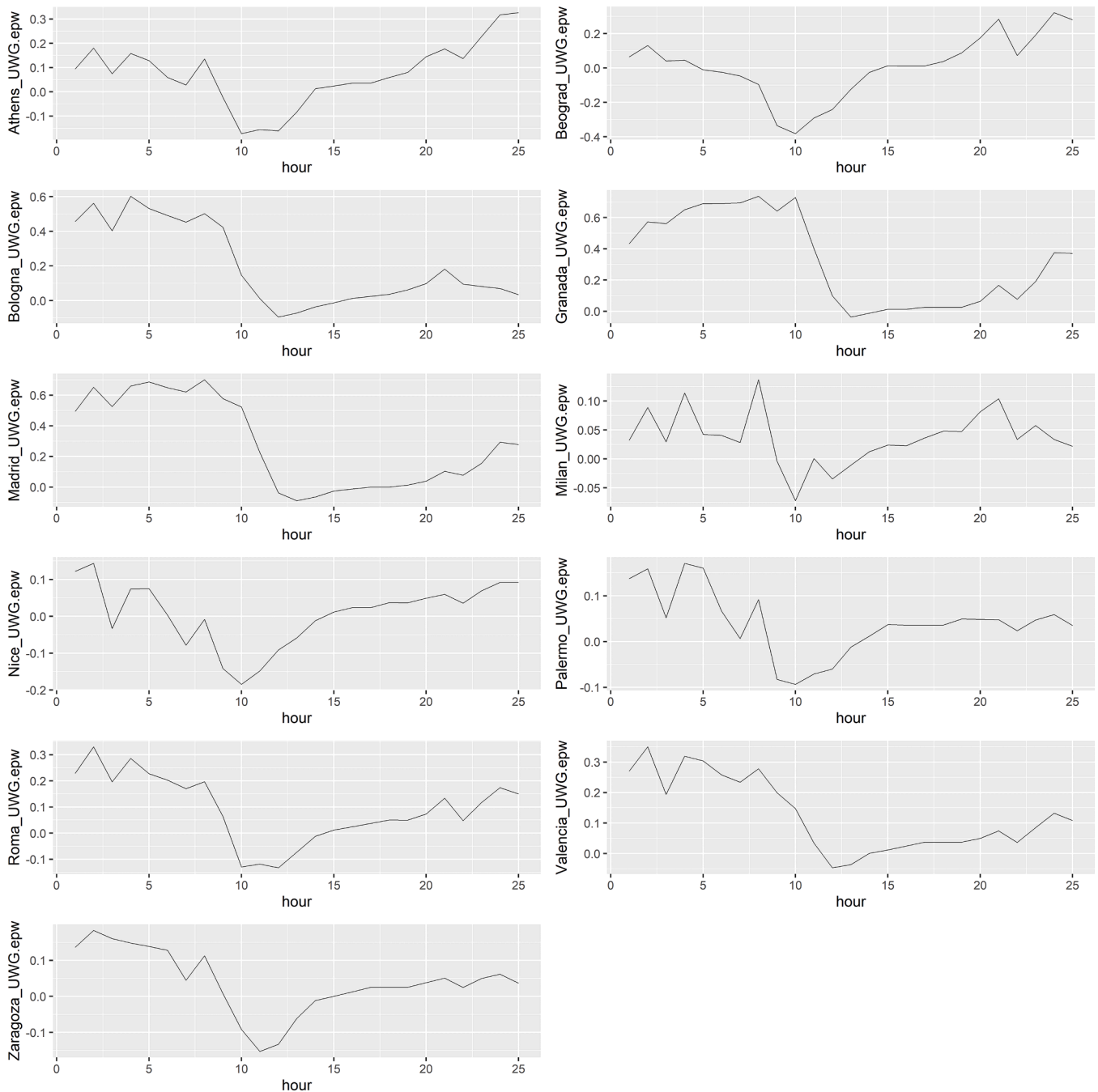


Fig. 8. Hourly delta between MOCI values in urban and rural areas for the different towns (30th of July).

intermittent activation was not counterbalanced by the energy and water consumption reduction (−40%).

For each configuration, VAR_{MOCI} , I_{energy} and I_{water} were calculated and analysed to evaluate the effectiveness of the specific technological choices (nozzle arrangement and presence of sun/wind shieldings) in each location.

Finally, VAR_{MOCI} , I_{energy} and I_{water} were combined to obtain a synthetic sustainability index for each climate/configuration, expressing the daily amount of energy and water (mean of the June–September period corresponding to 120 days) required to obtain a unitary variation of the MOCI value:

$$S_e = \frac{I_{energy}}{VAR_{MOCI} * 120} \text{ [kWh / m}^2\text{*day]} \tag{7}$$

$$S_w = \frac{I_{water}}{VAR_{MOCI} * 120} \text{ [l*h / m}^2\text{*day]} \tag{8}$$

In some cases, the spray cooling device cannot obtain a unitary variation of the $MOCI_{out}$, then S_e and S_w express the normalized consumption and not to the real expected consumption. All calculations were performed through scripts written in R statistics programming language (rel. 4.3) and necessary packages.

3. Results

3.1. Analysis of MOCI data

Based on experimental data, the MOCI index has been calculated

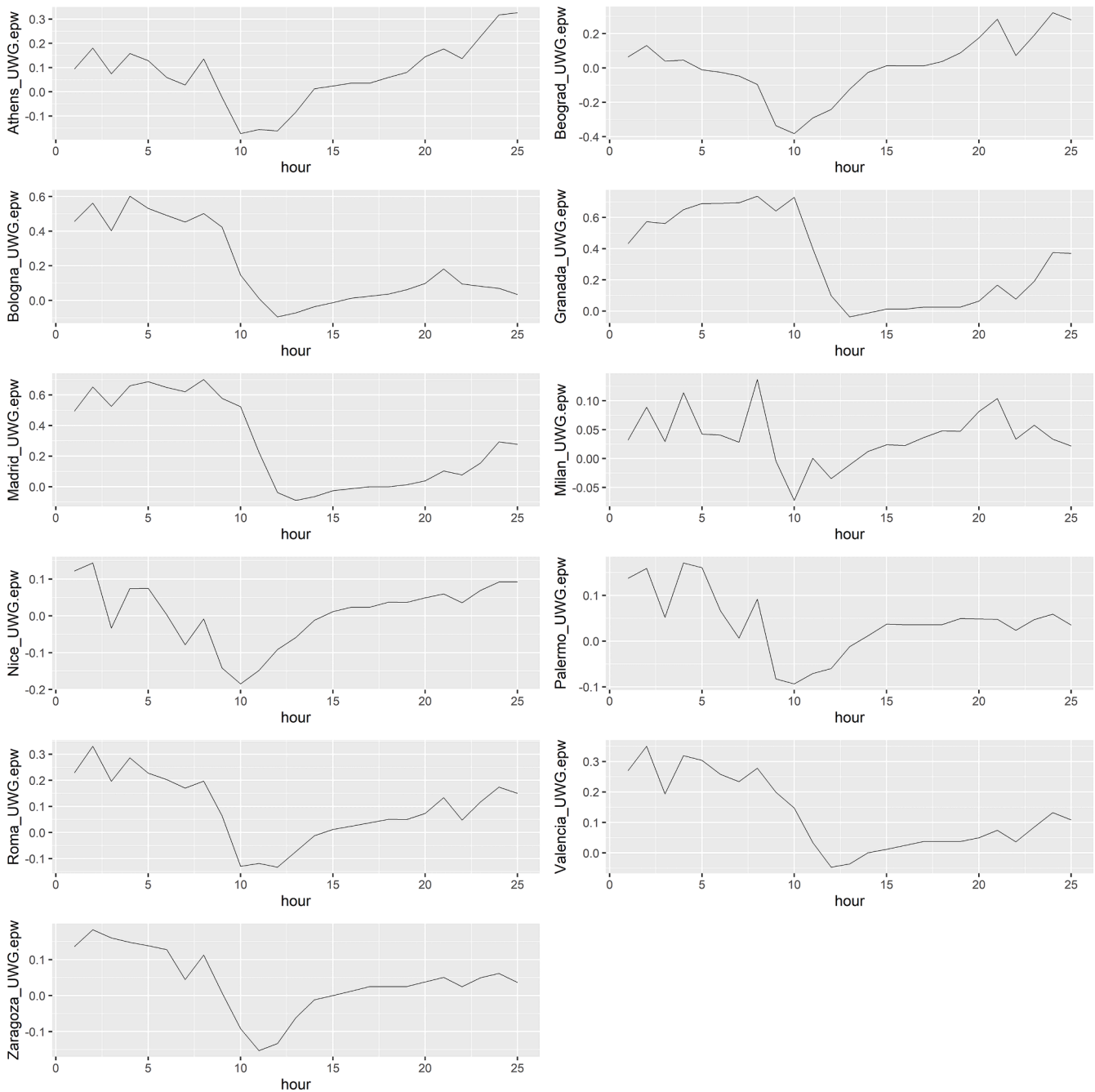


Fig. 8. (continued).

both for the UC ($MOCI_{out}$) and for the 4 areas below the spray cooling apparatus ($MOCI_{in,1}$, $MOCI_{in,2}$, $MOCI_{in,3}$, $MOCI_{in,4}$). The mean of $MOCI_{1,2,3,4}$ has been also calculated ($MOCI_{in,mean}$). $MOCI_{out}$ values range from -2.53 to 2.10 , the 1st quartile is -0.38 , the median is $0,03$, and the 3rd quartile is 0.56 . Fig. 4 shows the global effect of the spray cooling device activity, expressed as boxplots of MOCI values in UC and MC.

When the apparatus is active, the MOCI values under the sprayed area are lower than $MOCI_{out}$. The median value shifts from 0.03 ($MOCI_{out}$) to -0.17 ($MOCI_{in,mean}$). The mean value shifts from -0.09 ($MOCI_{out}$) to -0.02 ($MOCI_{in,mean}$). The quartile distribution of the MOCI values recorded in the four different areas is quite similar. The delta between $MOCI_{in,mean}$ and $MOCI_{out}$ is mainly negative when the $MOCI_{out}$ values are positive (warm or hot conditions).

The influence of the meteorological parameters on MOCI (in both UC

and MC) is analysed through the scatterplots reported in Fig. 5, representing MOCI values (y-axis) versus T_A , RH, I_s , WS (x-axis). $MOCI_{out}$ is directly correlated to T_A and I_s while inversely correlated to RH and WS. Scatterplots related to $MOCI_{in}$ represent different clouds of points partially overlapped, depending on the different configurations assumed by the spray system (nozzle position, presence of shieldings) during the monitoring period.

3.2. LSTM RNN accuracy

At the end of the training process, the LSTM Neural Network’s ability to predict MOCI values was evaluated through two metrics, “loss” and “mean absolute error”, whose respective obtained values were 0.012 and 0.059 , demonstrating the ability of the trained RNN to predict MOCI values with high accuracy. Fig. 6 shows the results of the testing process.

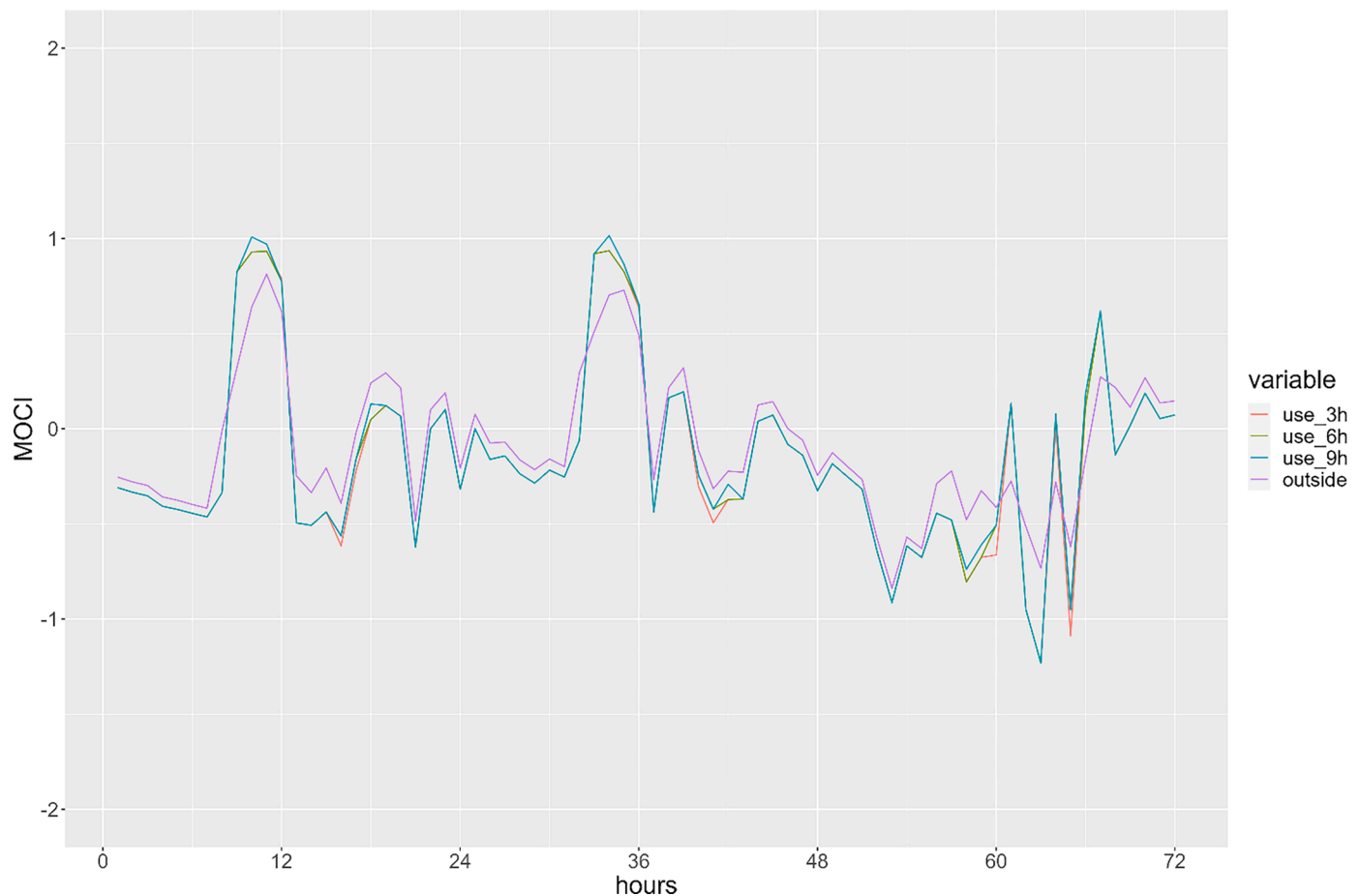


Fig. 9. Predicted MOCI values in UC and MC for the city of Athens during three days of the last week of July, with the following mist system settings: nozzle height 2.2 m, no sun/wind shielding, 3 different daily activation periods of the system, “use_3h”= spray cooling on from 11 to 14; “use_6h”= spray cooling on from 11 to 16, “use_9h”= spray cooling on from 9 to 17.

Original and predicted MOCI values are almost totally overlapped, with very limited differences when the highest and the lowest MOCI values were recorded.

3.3. Urban weather files

To evaluate the impact of the introduction of the spray cooling device in different urban contexts, a set of “urban” weather files has been generated through UWG software covering the period from June to September (120 days). For each of the 11 considered towns, the hourly MOCI values were calculated both in the rural area (based on the original rural EPW files) and in the urban area at canyon level (based on the obtained urban EPW files).

Fig. 7 shows the distributions of the difference between the two calculated MOCI values for each town, i.e.: MOCI urban value - MOCI rural value. As expected, the urban climate corresponding to LCZ2 affects the MOCI values of every town, shifting the values towards warm and hot perceptions. Fig. 8 represents the hourly trend of this “delta MOCI” for each town on a typical summer day (end of July). It is possible to observe that, in the urban areas, MOCI values are higher compared to rural ones, especially in the afternoon and in the first part of the night, in coherence with the existing literature (Oke, Mills, Christen, & Voogt, 2017).

3.4. MOCI prediction through the LSTM RNN

Through the LSTM RNN, MOCI time-series values from June to September (120 days) in MC for each town and each mist system

configuration were predicted. By way of example, Fig. 9 shows the predicted MOCI values inside and outside the sprayed area for the city of Athens during three days of the last week of July, considering 3 different daily activation periods of the mist system (3h:12–14, 6h:11–16, 9h:9–17).

It is possible to observe a drastic reduction of MOCI values in MC compared to the MOCI outside after the activation of the system, especially in the middle part of the day, when air temperature and global irradiation reach the peak. However, considering that MOCI is also influenced by relative humidity, which is increased by the water mist spray, and by wind speed, differences between the MOCI values in MC and UC are reduced in the phase of the day with decreasing temperatures. The small differences between MOCI values in MC and UC still visible when the mist spray system is inactive are due to the accuracy of the trained Neural Network.

Fig. 10 shows the mean and variance of $MOCI_{in}$ (red points) with respect to the $MOCI_{out}$ (blue points), for each design configuration and town, during the simulated period of 120 days. As expected, the spray cooling device causes a reduction of the mean MOCI values (cooling effect), but not for all the configurations analysed. The maximum recorded shift of the mean value is about 1. Considering that we analysed only periods with $MOCI > 1$, the spray cooling device allows reaching thermal conditions between neutral and slightly warm. The variance is quite limited and between 0.05 and 0.15. It can be observed that there are cases characterized by an increase in the mean MOCI in MC.

A major detail on the role given by the design solutions on MOCI variations is provided in Fig. 11 and Fig. 12.

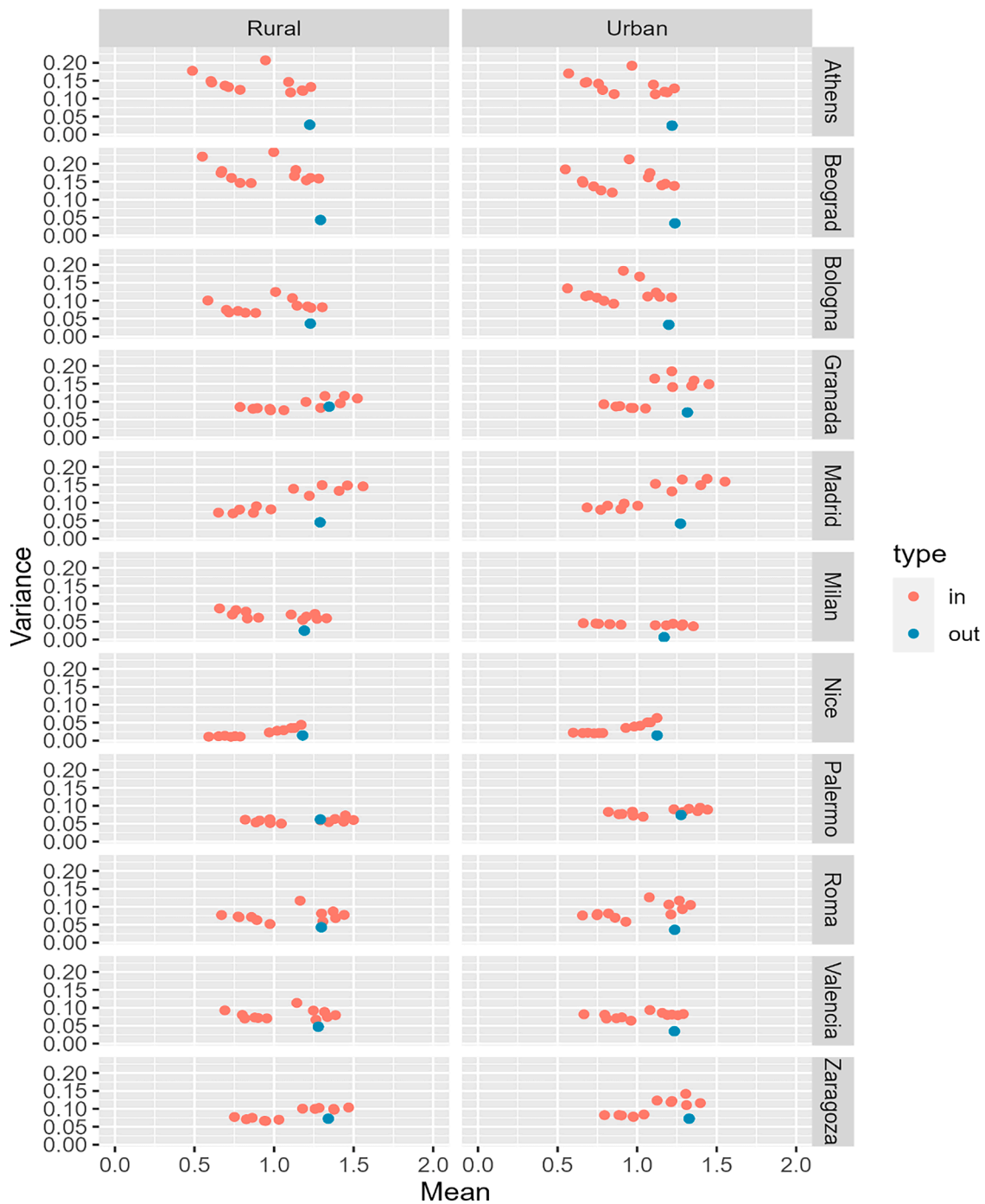


Fig. 10. Mean and Variance of predicted MOCI values below and outside the spray cooling areas for all the towns, both in urban and rural areas, and for all considered design variants when the spray cooling is active. Legend: “In”= MOCI_{in} (red points); “Out”: MOCI_{out} (blue points).(For interpretation of the references to color in this figure legend, the reader is referred to the web version of this article.)

In particular, Fig. 11 represents the alternative scenarios with/without shieldings. The left column represents the value obtained without the upper shielding protection. The right column represents the value obtained with the upper shielding protection. The first row represents the value obtained without lateral wind protection. The second row represents the value obtained with the lateral wind protection. When the sun/wind shieldings are installed, there is a clear shift towards negative MOCI values (cool). On the contrary, when no protection devices are installed, we can observe in some cases a little shift (< 0.2) towards positive values. This fact is probably due to the dilution effect of the wind reported by some authors: wind can move the moist air outside

the spray cooling area, reducing the cooling effect below the nozzles (Ulpiani, 2019).

Fig. 12 focuses on the height of the nozzles (values reported in the lines of the graphs). It demonstrates how the reduction of the height of the nozzles from 2.9 m to 2.2 m decreases the mean MOCI values below the apparatus, due to the reduced effect of wind washing.

3.5. Climate benefits vs energy and water consumption

The benefits of the spray cooling device have been evaluated through the synthetic index VAR_{MOCI} and compared to the resources

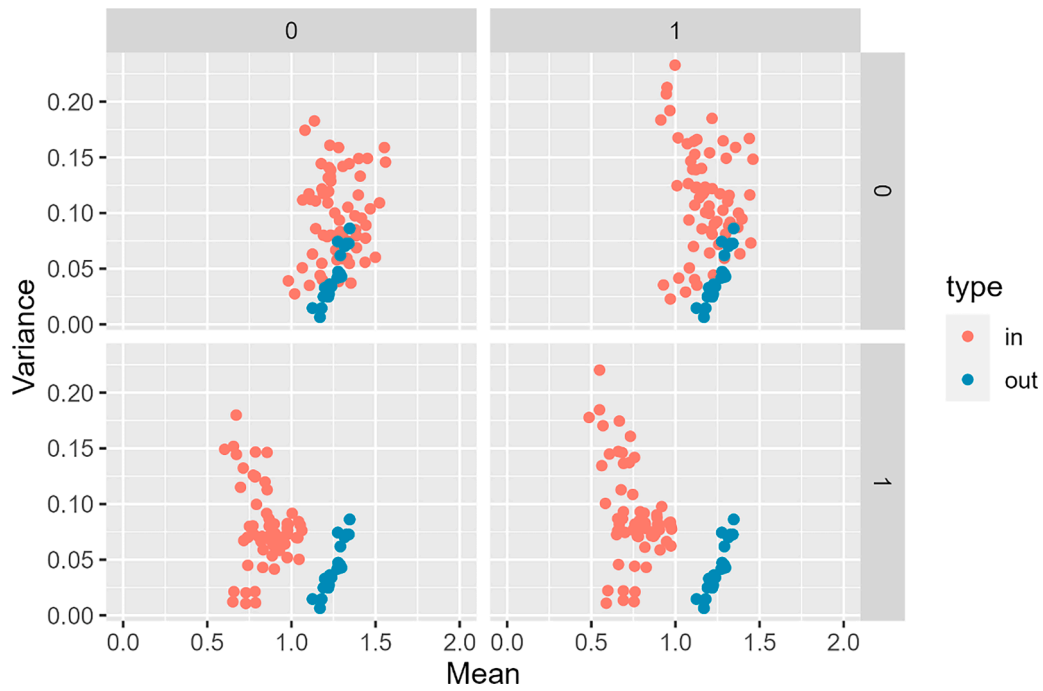


Fig. 11. Mean and Variance of predicted MOCI values below and outside the spray cooling areas for all the towns and for all considered combinations when the spray cooling is active. Legend: “In”= $MOCI_{in}$ (red points); “Out”: $MOCI_{out}$ (blue points). (For interpretation of the references to colour in this figure legend, the reader is referred to the web version of this article.)

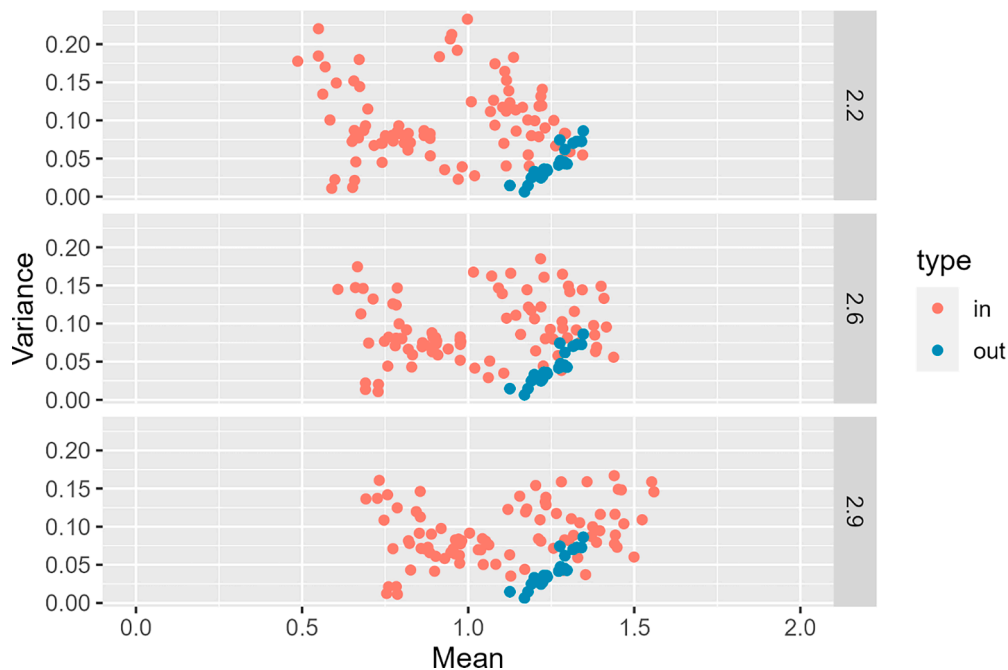


Fig. 12. Mean and Variance of predicted MOCI values below and outside the spray cooling areas for all the towns and for all considered combinations when the spray cooling is active. Legend: “In”= $MOCI_{in}$ (red points); “Out”: $MOCI_{out}$ (blue points). (For interpretation of the references to colour in this figure legend, the reader is referred to the web version of this article.)

consumptions I_{energy} (Fig. 13) and I_{water} (Fig. 14), for each of the analysed mist configuration (height of the nozzles and presence/absence of lateral and upper shieldings) in each town. In the figures, the rows express the different heights of the nozzles, the first column the absence of shieldings, the second column the presence of an upper shielding (1 = true; 0 = false), the third column the presence of a side shielding (1 = true; 0 = false), the fourth column the presence of both side and upper

shieldings. For each configuration and town, a different functioning time is obtained, considering that the spray cooling device was activated only for $MOCI_{out} > 1$.

It is possible to observe that the presence of upper and lateral shieldings has a strong impact on the obtainable benefits. Without shieldings, in all towns, benefits are very limited, especially when the nozzles are far from the human body. The introduction of upper and side

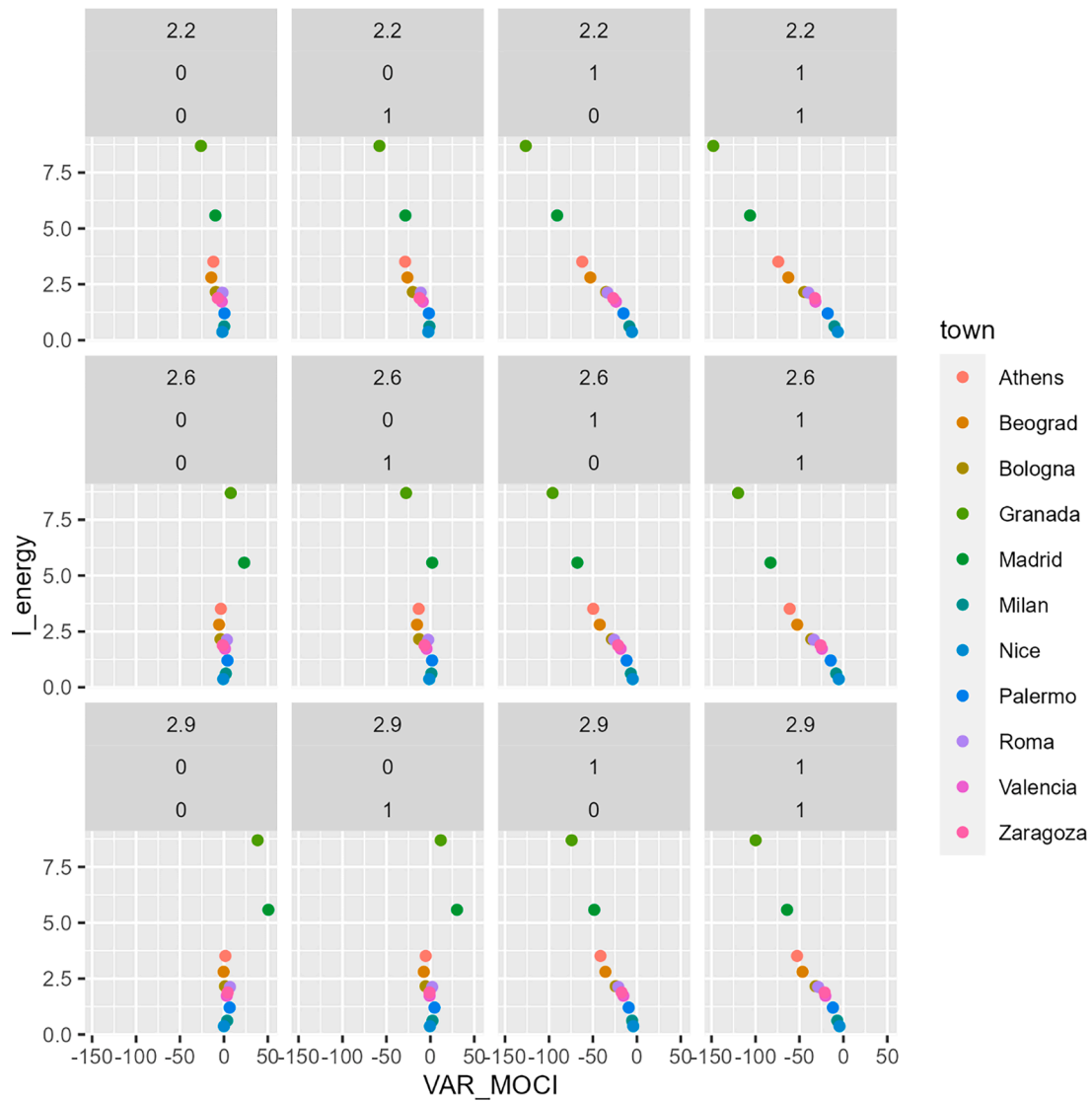


Fig. 13. VAR_{MOCI} values for each system configuration with respect to the cumulative energy consumption (I_{energy}) in each town (represented by colours). (For interpretation of the references to colour in this figure legend, the reader is referred to the web version of this article.)

shieldings increases the benefits, especially when the height of the nozzles is low (2.2 m). In those cases, VAR_{MOCI} shifts towards negative values, confirming the positive influence of the spray cooling system. Benefits are bigger in the towns characterized by the hottest climate (such as Granada, Madrid and Athens). The energy and water consumptions differ in the different towns considering the different activation periods due to the limitation to MOCI > 1, for a maximum of 9 h/day.

The energy required during the considered period (June-September) to improve outdoor comfort through spray cooling systems ranges from 0.37 to 8.70 kWh/m² (Fig. 13). Assuming a people density of 2 people/m², the personal consumption ranges from 0.18 to 4.35 kWh. The required water varies from 57 to 1340 l/m², i.e. 28–670 l/person (0.03–0.67 mc/person). The lowest consumptions (energy and water) are obtained for the towns where the cooling benefits are bigger. This is because the spray cooling device has constant hourly energy and water consumption, then the cumulative consumption only depends on the functioning time. There are towns, such as Nice, where the benefits are very limited not justifying the activation of the system.

3.6. Sustainability of spray cooling applications

Obtained results can be useful to evaluate the ratio between the cooling benefit and the environmental costs of spray cooling systems in different climate zones and towns. Table 3 shows S_e and S_w values, expressing the amount of energy and water daily required to obtain a unitary variation of MOCI towards neutrality.

Considering that in some cases the spray cooling device cannot obtain a unitary variation of MOCI, S_e and S_w express the normalized daily consumption and not the real expected daily consumption. The daily real expected consumption can be obtained by dividing I_{energy} and I_{water} by 120 (functioning period in days). Cases characterized by the worsening of outdoor MOCI values are omitted (empty cells).

The mean value of the energy required to obtain a unitary MOCI variation in all considered cases is 4,17 Wh/m²*day. When the nozzles are installed near the human body and when upper and lateral protection devices are installed, the energy required to obtain a unitary MOCI variation falls below 0,56 kWh/day*person. The mean value of the water required by the spray cooling device to obtain a unitary MOCI variation is 0,56 l*h/m²*day.

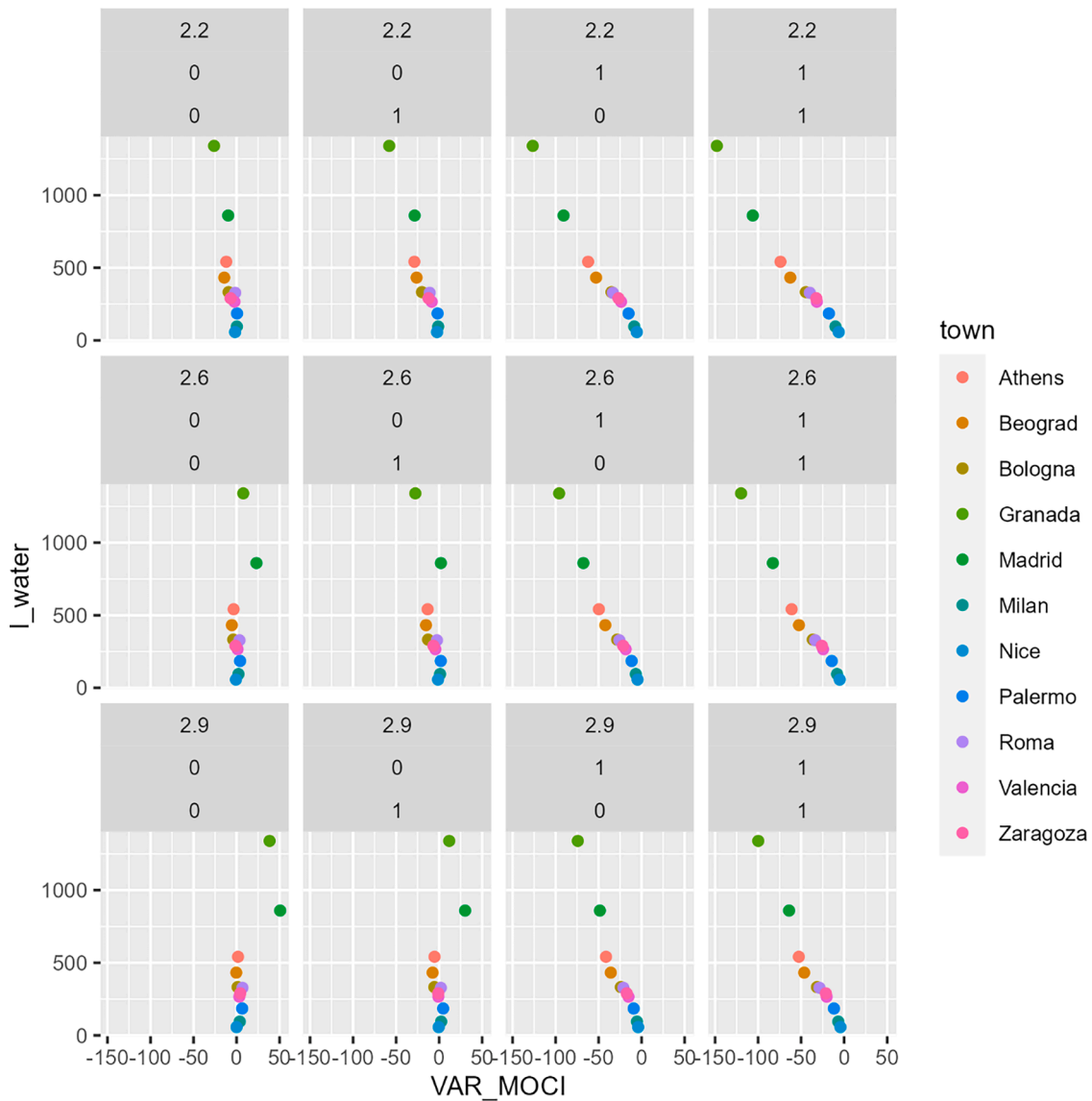


Fig. 14. VAR_{MOCI} values for each system configuration with respect to the cumulative water consumption (I_{water}) in each town (represented by colours). (For interpretation of the references to colour in this figure legend, the reader is referred to the web version of this article.)

4. Discussion

Water spraying contribution to the enhancement of outdoor well-being and health is well documented in the literature (Ulpiani, 2019). Results obtained in this study confirm that spray cooling reduces MOCI, thus improving outdoor comfort, in almost all simulated cases.

However, results also demonstrate that design arrangements strongly affect results. Indeed, without lateral wind and upper sun shieldings, and with a great nozzle's height (2.9 m), the wind dilution effect reduces the cooling efficiency. Several authors already showed how misting systems in open spaces are sensitive to the airflow rate (Di Giuseppe et al., 2021; Jun-feng & Xin-cheng, 2009; Ulpiani, 2019; Wang, Tu, Wang, & Huang, 2010).

Even if mist spray cooling is beneficial for human outdoor comfort, the environmental costs, in terms of resources consumptions, are not negligible, especially with the recent diffusion of systems based on continuous use and without activation logics based on real needs (climatic conditions and the presence of a suitable number of people to satisfy).

Considering that the proportion of land allocated to streets and public squares in European Union cities ranges from 14% to 33%

(Warah, 2013), even assuming a limited portion of them intended for spray cooling applications, the related energy and water consumptions can be great. For instance, in Rome (2,800,000 inhabitants), assuming only 1% of the land allocated to streets and public square intended for spray cooling applications, energy and water consumption for mist cooling during the summer period could reach respectively 5.450 kWh and 96.000 mc.

These considerations confirm the need of control logics able to optimize the ratio between benefits and costs. Also according to the guidelines provided in the extensive literature review of Ulpiani, misting should be stopped whenever T_A is below 30 °C, RH over 70%, and WS over 3 m/s; and windscreens should be provided to limit wind dilution (Ulpiani, 2019).

Moreover, water recovering technologies should be considered, especially in countries with limited resources, to ensure the use at a large scale.

This study is based on a Neural Network trained on experimental data, assuming specific configurations, then, to further generalize the results, it is necessary to extend the experimental activities to other configurations and train the Neural Network with extended datasets.

Table 3

Mean daily value (in the period June–September) of the energy and water required to obtain a unitary decrease of the outdoor MOCI. Energy is expressed in Wh/m²*day. Water is expressed in l*h/(m²*day).

Se (Wh/m ² *day)													
Nozzle height	Upper protection	Lateral protection	Bsk		Csa							Csb	
			Granada	Valencia	Zaragoza	Athens	Beograd	Madrid	Nice	Palermo	Roma	Bologna	Milan
2,2	1	1	0,49	0,45	0,48	0,40	0,37	0,44	0,49	0,56	0,44	0,40	0,51
	0	1	0,57	0,60	0,58	0,47	0,44	0,51	0,55	0,66	0,53	0,51	0,60
	1	0	1,25	1,67	1,27	1,02	0,89	1,64	1,31	5,78	1,61	0,90	4,65
	0	0	2,77	5,86	2,26	2,45	1,64	4,78	1,79		10,89	1,95	
2,6	1	1	0,60	0,59	0,60	0,48	0,45	0,56	0,59	0,69	0,53	0,49	0,62
	0	1	0,76	0,78	0,73	0,59	0,55	0,69	0,65	0,86	0,69	0,63	0,76
	1	0	2,62	3,37	2,38	2,20	1,54		2,43		7,05	1,40	
	0	0			12,10	8,59	4,25		4,24			4,65	
2,9	1	1	0,73	0,71	0,73	0,56	0,50	0,73	0,70	0,84	0,62	0,57	0,75
	0	1	0,98	0,94	0,90	0,71	0,65	0,96	0,75	1,08	0,84	0,74	0,95
	1	0		16,49	15,61	5,50	3,11		6,06			3,24	
	0	0					65,23		451,96				

Sw (l*h/m ² *day)													
Nozzle height	Upper protection	Lateral protection	Bsk		Csa							Csb	
			Granada	Valencia	Zaragoza	Athens	Beograd	Madrid	Nice	Palermo	Roma	Bologna	Milan
2,2	1	1	0,07	0,06	0,07	0,05	0,05	0,06	0,07	0,08	0,06	0,05	0,07
	0	1	0,08	0,08	0,08	0,06	0,06	0,07	0,07	0,09	0,07	0,07	0,08
	1	0	0,17	0,23	0,17	0,14	0,12	0,22	0,18	0,78	0,22	0,12	0,63
	0	0	0,37	0,79	0,31	0,33	0,22	0,65	0,24		1,47	0,26	
2,6	1	1	0,08	0,08	0,08	0,06	0,06	0,08	0,08	0,09	0,07	0,07	0,08
	0	1	0,10	0,11	0,10	0,08	0,07	0,09	0,09	0,12	0,09	0,09	0,10
	1	0	0,35	0,46	0,32	0,30	0,21		0,33		0,95	0,19	
	0	0			1,63	1,16	0,57		0,57			0,63	
2,9	1	1	0,10	0,10	0,10	0,08	0,07	0,10	0,10	0,11	0,08	0,08	0,10
	0	1	0,13	0,13	0,12	0,10	0,09	0,13	0,10	0,15	0,11	0,10	0,13
	1	0		2,23	2,11	0,74	0,42		0,82			0,44	
	0	0					8,82		61,08				

5. Conclusion

This study analyses the effectiveness and sustainability of water mist spray devices installed in the Mediterranean area, providing benefits (outdoor cooling) and environmental loads (energy and water consumption) in 22 different rural and urban settings, referred to 11 cities in the Mediterranean area. Based on experimental data collected on a water mist system, a Long-Short-Term-Memory Recurrent Neural Network has been trained to predict Mediterranean Outdoor Comfort Index values in the sprayed area under several design arrangements concerning nozzles heights and the presence of side and upper shieldings. The trained LSTM RNN was tested obtaining high accuracy (mean absolute error < 0.059), and then applied to microclimate models of 11 cities, to predict the variation of MOCI due to the specific arrangements and climate contexts and the needed energy and water resources.

Indeed, the issue of environmental loads for water misting solutions,

more and more used in every-day life applications in developed countries (i.e. open urban places, amusement parks, concerts, etc.), needs to be urgently addressed to limit the impacts. Despite the amount of research on water mist performance, the environmental sustainability of this technology is still a relatively unexplored issue, for the first time treated in this contribution.

Results show that when sun/wind shieldings are used in the sprayed area, or the height of nozzles is limited, cooling results are more easily achieved. However, energy and water consumption are extremely high if misting systems are perennially active during the day. These results confirm the need of mandatory regulations for misting applications managed by control logics based on the acquisition of climatic data in real time, in order to limit resources consumption.

Declaration of Competing Interest

The authors declare that they have no known competing financial interests or personal relationships that could have appeared to influence the work reported in this paper.

Data availability

Data will be made available on request.

References

- Bao, J., Wang, Y., Xu, X., Niu, X., Liu, J., & Qiu, L. (2019). Analysis on the influences of atomization characteristics on heat transfer characteristics of spray cooling. *Sustainable Cities and Society*, 51(March), Article 101799. <https://doi.org/10.1016/j.scs.2019.101799>
- Boccalatte, A., Fossa, M., Gaillard, L., & Menezo, C. (2020). Microclimate and urban morphology effects on building energy demand in different European cities. *Energy and Buildings*, 224, Article 110129. <https://doi.org/10.1016/j.enbuild.2020.110129>
- Bueno, B., Nakano, A., & Norford, L. (2015). Urban weather generator : A method to predict neighborhood-specific urban temperatures for use in building energy simulations. In *ICUC9 - 9th International Conference on Urban Climate Jointly with 12th Symposium on the Urban Environment*.
- Burak Gunay, H., Shen, W., & Newsham, G. (2019). Data analytics to improve building performance: A critical review. *Automation in Construction*, 97, 96–109. <https://doi.org/10.1016/j.autcon.2018.10.020>
- Coccia, G., Summa, S., Di Giuseppe, E., D'Orazio, M., Zinzi, M., & Di Perna, C. (2023). Experimental evaluation of a water spray system for semi-outdoor spaces: Analysis of the effect of the operational parameters. *Building and Environment*, 241(January), Article 110456. <https://doi.org/10.1016/j.buildenv.2023.110456>
- Cohen, M., Corff, S. Le, Charbit, M., Champagne, A., Nozière, G., & Preda, M. (2021). End-to-end deep meta modelling to calibrate and optimize energy consumption and comfort. *Energy and Buildings*, 250, Article 111218. <https://doi.org/10.1016/j.enbuild.2021.111218>
- Desert, A., Naboni, E., & Garcia, D. (2020). The spatial comfort and thermal delight of outdoor misting installations in hot and humid extreme environments. *Energy and Buildings*, 224, Article 110202. <https://doi.org/10.1016/j.enbuild.2020.110202>
- Di Giuseppe, E., Ulpiani, G., Cancellieri, C., Di Perna, C., D'Orazio, M., & Zinzi, M. (2021). Numerical modelling and experimental validation of the microclimatic impacts of water mist cooling in urban areas. *Energy and Buildings*, 231, Article 110638. <https://doi.org/10.1016/j.enbuild.2020.110638>
- Falasca, S., Curci, G., & Salata, F. (2021). On the association between high outdoor thermo-hygrometric comfort index and severe ground-level ozone: A first investigation. *Environmental Research*, 195, Article 110306. <https://doi.org/10.1016/j.envres.2020.110306>
- Farnham, C., Emura, K., & Mizuno, T. (2015a). Evaluation of cooling effects: Outdoor water mist fan. *Building Research & Information*, 43(3), 334–345. <https://doi.org/10.1080/09613218.2015.1004844>
- Farnham, C., Nakao, M., Nishioka, M., Nabeshima, M., & Mizuno, T. (2015b). Effect of water temperature on evaporation of mist sprayed from a nozzle. *Journal of Heat Island Institute International*, 10, 35–44.
- Gonçalves, P., Araújo, M., Benevenuto, F., & Cha, M. (2013). Comparing and combining sentiment analysis methods. In *COSN 2013 - Proceedings of the 2013 Conference on Online Social Networks* (pp. 27–37). <https://doi.org/10.1145/2512938.2512951>
- Jun-feng, W., & Xin-cheng, T. (2009). Experimental study and numerical simulation on evaporative cooling of fine water mist in outdoor environment. *2009 International Conference on Energy and Environment Technology*, 156–159. <https://doi.org/10.1109/ICEET.2009.44>
- Kachhwaha, S. S., Dhar, P. L., & Kale, S. R. (1998). Experimental studies and numerical simulation of evaporative cooling of air with a water spray - I. Horizontal parallel flow. *International Journal of Heat and Mass Transfer*, 41(2), 447–464. [https://doi.org/10.1016/S0017-9310\(97\)00133-6](https://doi.org/10.1016/S0017-9310(97)00133-6)
- Li, Y., Hong, B., Wang, Y., Bai, H., & Chen, H. (2022). Assessing heat stress relief measures to enhance outdoor thermal comfort: A field study in China's cold region. *Sustainable Cities and Society*, 80, Article 103813. <https://doi.org/10.1016/j.scs.2022.103813>
- Litardo, J., Palme, M., Borbor-Cordova, M., Caiza, R., Macias, J., Hidalgo-Leon, R., & Soriano, G. (2020). Urban Heat Island intensity and buildings' energy needs in Duran, Ecuador: Simulation studies and proposal of mitigation strategies. *Sustainable Cities and Society*, 62(February), Article 102387. <https://doi.org/10.1016/j.scs.2020.102387>
- Mao, H., Meng, Q., Li, S., Qi, Q., Wang, S., & Wang, J. (2021). Cooling effects of a mist-spraying system on ethylene tetrafluoroethylene cushion roofs in hot-humid areas: A case study in Guangzhou, China. *Sustainable Cities and Society*, 74(July), Article 103211. <https://doi.org/10.1016/j.scs.2021.103211>
- Mao, J., Fu, Y., Afshari, A., Armstrong, P. R., & Norford, L. K. (2018). Optimization-aided calibration of an urban microclimate model under uncertainty. *Building and Environment*, 143(April), 390–403. <https://doi.org/10.1016/j.buildenv.2018.07.034>
- Maracchini, G., Bavarsad, F. S., Di Giuseppe, E., & D'Orazio, M. (2023). Sensitivity and uncertainty analysis on Urban Heat Island intensity using the local climate zone (LCZ) schema: The case study of Athens. *Sustainability in energy and buildings* (pp. 281–290). Singapore: Springer. https://doi.org/10.1007/978-981-19-8769-4_27
- Meng, X., Meng, L., Gao, Y., & Li, H. (2022). A comprehensive review on the spray cooling system employed to improve the summer thermal environment: Application efficiency, impact factors, and performance improvement. *Building and Environment*, 217, Article 109065. <https://doi.org/10.1016/J.BUILDENV.2022.109065>
- Nakano, A., Bueno, B., Norford, L., & Reinhart, C. F. (2015). Urban weather generator - A novel workflow for integrating Urban Heat Island effect within urban design process. In *14th International Conference of IBPSA - Building Simulation 2015, BS 2015, Conference Proceedings, (December 2017)* (pp. 1901–1908).
- Nishimura, T., Rashed, E. A., Koderia, S., Shirakami, H., Kawaguchi, R., Watanabe, K., ... Hirata, A. (2021). Social implementation and intervention with estimated morbidity of heat-related illnesses from weather data: A case study from Nagoya City, Japan. *Sustainable Cities and Society*, 74(May), Article 103203. <https://doi.org/10.1016/j.scs.2021.103203>
- Oke, T. R., Mills, G., Christen, A., & Voogt, J. A. (2017). *Urban climates*. Cambridge: Cambridge University Press. <https://doi.org/10.1017/9781139016476>
- Ribeiro, F. N., Araújo, M., Gonçalves, P., André Gonçalves, M., & Benevenuto, F. (2016). SentiBench - a benchmark comparison of state-of-the-practice sentiment analysis methods. *EPJ Data Science*, 5(1), 1–29. <https://doi.org/10.1140/epjds/s13688-016-0085-1>
- Salata, F., Golasi, I., de Lieto Vollaro, R., & de Lieto Vollaro, A. (2016). Outdoor thermal comfort in the Mediterranean area. A transversal study in Rome, Italy. *Building and Environment*, 96, 46–61. <https://doi.org/10.1016/j.buildenv.2015.11.023>
- Santamouris, M., Ding, L., Fiorito, F., Oldfield, P., Osmond, P., Paolini, R., & Synnefa, A. (2017). Passive and active cooling for the outdoor built environment – Analysis and assessment of the cooling potential of mitigation technologies using performance data from 220 large scale projects. *Solar Energy*, 154, 14–33. <https://doi.org/10.1016/j.solener.2016.12.006>
- Santamouris, M., & Kolokotsa, D. (2016). Urban climate mitigation techniques. In D. Kolokotsa (Ed.), *Mat Santamouris*. London: Routledge.
- Singh, S., Singh, D. S., & Kumar, S. (2014). Modified mean square error algorithm with reduced cost of training and simulation time for character recognition in backpropagation neural network. *Advances in Intelligent Systems and Computing*, 247, 137–145. https://doi.org/10.1007/978-3-319-02931-3_17
- Ulpiani, G. (2019). Water mist spray for outdoor cooling: A systematic review of technologies, methods and impacts. *Applied Energy*, 254(August), Article 113647. <https://doi.org/10.1016/j.apenergy.2019.113647>
- Ulpiani, G., Di Giuseppe, E., Di Perna, C., D'Orazio, M., & Zinzi, M. (2019a). Design optimization of mist cooling for Urban Heat Island mitigation: Experimental study on the role of injection density. *IOP Conference Series: Earth and Environmental Science*, 296(1), Article 012025. <https://doi.org/10.1088/1755-1315/296/1/012025>
- Ulpiani, G., Di Giuseppe, E., Di Perna, C., D'Orazio, M., & Zinzi, M. (2019b). Thermal comfort improvement in urban spaces with water spray systems: Field measurements and survey. *Building and Environment*, 156(April), 46–61. <https://doi.org/10.1016/j.buildenv.2019.04.007>
- Vanos, J. K., Wright, M. K., Kaiser, A., Middel, A., Ambrose, H., & Hondula, D. M. (2022). Evaporative misters for urban cooling and comfort: Effectiveness and motivations for use. *International Journal of Biometeorology*, 66(2), 357–369. <https://doi.org/10.1007/s00484-020-02056-y>
- Wang, J., Tu, X., Wang, Z., & Huang, J. (2010). Application and numerical simulation on water mist cooling for urban environment regulation, 98. *Lecture notes in computer science*. Berlin, Heidelberg: Springer. https://doi.org/10.1007/978-3-642-15615-1_55
- Warah, R. (2013). *Streets as public spaces and drivers of urban prosperity*. Nairobi: UN Habitat.
- Zheng, K., Yuan, C., Wong, N. H., & Cen, C. (2019). Dry mist systems and its impact on thermal comfort for the tropics. *Sustainable Cities and Society*, 51, Article 101727. <https://doi.org/10.1016/j.scs.2019.101727>